

Chaotic Motion of a Tethered Satellite System

J. H. Peng, Y. Z. Liu

The use of tethered satellites has been proposed and implemented in a few instances. It is a device to extend the capability of spacecraft to perform scientific and application investigations. The present paper discusses the libration and longitude vibration of a tethered satellite system. By the analytical method of Melnikov and the numerical calculation of Poincaré maps, it is observed that this system's motion may become chaotic.

1 Introduction

The use of tethered satellite has been proposed for space exploitation and development. It is a device to extend e. g. the capability of the Space Shuttle to perform scientific and application investigations. The subsatellite is suspended from the Shuttle cargo bay, toward or away from the Earth, at distances up to 100 kilometers from the Shuttle. The dynamics and control of this system have received considerable attention in the past few years. The interest is focused on the deployment and retrieval of the subsatellite, the vibration and libration control, station keeping et al. The present paper discusses the plane swing and longitudinal vibration of a tethered satellite system. By the analytical method of Melnikov and numerical calculation of Poincaré surfaces of section, it is observed that this system may perform a chaotic motion. When the longitudinal elastic tether displacement is assumed to be small, according to Liu (1992) the tether behaves like a sinusoidal vibrating string, and can be taken as a system of one degree of freedom with periodic perturbation. When the longitudinal elastic tether displacement is large, the plane swing and longitudinal displacement are strongly coupled, we take it as a system of two degrees of freedom.

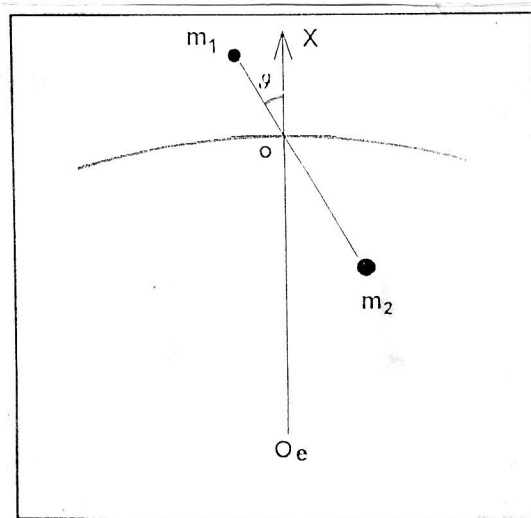


Figure 1. Mass m_1 and tethered submass m_2

2 Planar Swing Excited by Periodic Varying Parameter

The system is idealized as two point masses connected by a massless elastic tether with mass center O of the system moving on a circular orbit with the angular velocity of ω_c . Assume that O_e is the center of the Earth, $O_e X$ is along the vector $O_e O$, ϑ is the pitch angle, l is the distance between m_1 and m_2 (see Figure 1), the equation of planar motion is given as (Bainum, 1980)

$$\ddot{\vartheta} + 2\left(\frac{\dot{l}}{l}\right)(\dot{\vartheta} + \omega) + 3\omega^2 \sin \vartheta \cos \vartheta = 0 \quad (1)$$

When longitudinal vibration is relatively small, the displacement can be described approximately as $l = l_0 + A \cos \omega_0 t$, $\frac{\dot{l}}{l} = \frac{-A \sin \omega_0 t}{l_0 \sin \omega_0 t}$ when l_0 is the original length of the tether, A is the amplitude of vibration, ω_0 is the vibrating frequency.

Defining $\tau = \omega_0 t$, $\delta = \frac{\omega}{\omega_0}$, $\varepsilon = \frac{A}{l_0}$, we write the dimensionless equation as

$$\frac{d^2 \vartheta}{d\tau^2} - 2\varepsilon \left(\frac{d\vartheta}{d\tau} + \delta \right) \sin \tau + 3\delta^2 \sin \vartheta \cos \vartheta = 0 \quad (2)$$

We define $x_1 = \vartheta$, $x_2 = \frac{d\vartheta}{d\tau}$, and rename τ as t , then equation (2) can be written as

$$\dot{\mathbf{x}} = \mathbf{f}(\mathbf{x}) + \varepsilon \mathbf{g}(\mathbf{x}, t) \quad (3)$$

where

$$\mathbf{f}(\mathbf{x}) = \begin{bmatrix} x_2 \\ -3\delta^2 \sin x_1 \cos x_1 \end{bmatrix} \quad \text{and} \quad \mathbf{g}(\mathbf{x}, t) = \begin{bmatrix} 0 \\ 2(x_2 + \delta) \sin t \end{bmatrix}$$

For $\varepsilon = 0$, equation (3) represents a planar integrable Hamiltonian system,

$$\begin{aligned} \dot{x}_1 &= \frac{\partial H}{\partial x_2} & \dot{x}_2 &= \frac{-\partial H}{\partial x_1} \\ H &= \left(\frac{1}{2}\right)(x_2^2 + 3\delta^2 \sin^2 x_1) \end{aligned} \quad (4)$$

the Hamiltonian system possesses a hyperbolic saddle point $P_0\left(\frac{\pi}{2.0}\right)$, and a homoclinic orbit $\Gamma_0 = \{\mathbf{q}_0(t) | t \in R\}$ with

$$\mathbf{q}_0 = \begin{bmatrix} \sin^{-1} \tanh(\sqrt{3}\delta t) \\ \sqrt{3}\delta \operatorname{sech}(\sqrt{3}\delta t) \end{bmatrix} \quad (5)$$

Γ_0 is the intersection of the stable manifold $W_\varepsilon^s(P_\varepsilon)$ and unstable manifold $W_\varepsilon^u(P_\varepsilon)$ of the system. For sufficiently small $\varepsilon > 0$ the system still has a hyperbolic periodic orbit $\gamma_\varepsilon^0(t) = p_0 + 0(\varepsilon)$. Correspondingly, the Poincaré map defined by $P_\varepsilon^{t_0} : \Sigma^0 \rightarrow \Sigma^0$; $\Sigma^0 = \{(x, t) | t = [0, T]\}$ still has a hyperbolic saddle point $P_\varepsilon = P_0 + 0(\varepsilon^2)$ with stable and unstable manifolds $W_\varepsilon^s(P_\varepsilon)$ and $W_\varepsilon^u(P_\varepsilon)$. The distance in the Poincaré map between the manifolds $W_\varepsilon^s(P_\varepsilon)$ and $W_\varepsilon^u(P_\varepsilon)$ is measured by

$$d(t_0) = \frac{\varepsilon M(t_0)}{|\mathbf{f}(q_0(0))|} + O(\varepsilon^2) \quad (6)$$

here $M(t_0)$ is the Melnikov function. It is given by

$$M(t_0) = \int_{-\infty}^{\infty} \mathbf{f}(q_0(t)) \wedge \mathbf{g}(q_0(t+t_0)) dt \quad (7)$$

Substituting equation (5) into equation (7), we obtain

$$M(t_0) = 2\sqrt{3}\delta^2 \int_{-\infty}^{\infty} \operatorname{sech}(\sqrt{3}\delta t) \sin(t+t_0) dt + 3\delta^2 \int_{-\infty}^{\infty} \operatorname{sech}^2(\sqrt{3}\delta t) \sin(t+t_0) dt \quad (8)$$

The solution in terms of elliptic functions is

$$M(t_0) = 2\pi \left(\operatorname{sech} \frac{\pi}{2\sqrt{3}\delta} + \operatorname{csch} \frac{\pi}{2\sqrt{3}\delta} \right) \sin \frac{t_0}{2\sqrt{3}\delta} \quad (9)$$

where $M(t_0)$ is a function of t_0 , and there exist simple zeros, this means that the stable and the unstable manifold intersect transversally, the Smale horseshoe exists, and the system may perform a chaotic motion. In Figure 2, equation (3) is numerically integrated for 30 different initial conditions, the Poincaré map is defined as $\Sigma x(t_0) = \{(x_1(t), x_2(t)) | t = kT, k = 1, 2, \dots\}$. In Figure 2a, for fairly small ε , we see that most of the Poincaré map is fairly well covered by invariant tori, that is, most of the periodic and quasiperiodic motions are preserved, as we go on increasing ε , some tori break into chaotic trajectories in the sense that the successive points on Poincaré maps do not lie on a curve any more, but fill an area densely. In Figures 2a, b, c we can also see a hyperbolic point and homoclinic orbits connected to it, and the small region close to the separatrix is covered by chaotic trajectories. These features corroborate the result obtained previously by means of the Melnikov theory.

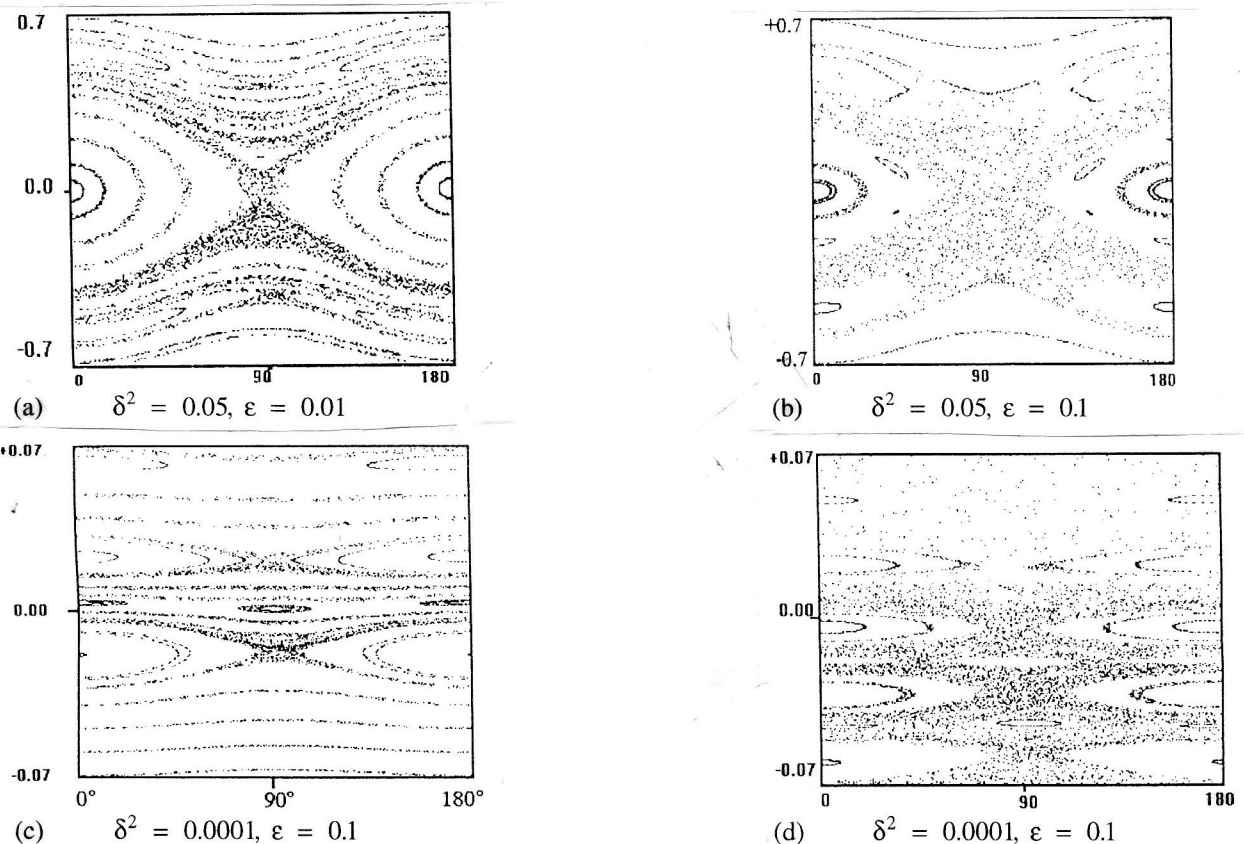


Figure 2. Poincaré maps $\Sigma x(t_0) = \{(x_1(t), x_2(t)) | t = kT, k = 1, 2, \dots\}$

3 The Coupled Motion of Swing and Longitudinal Displacement

When the longitudinal elastic tether displacement is large, the plane swing and longitudinal displacement are strongly coupled, and the system should be taken as having two degrees of freedom. The Hamiltonian of the system is (Bainum, 1980)

$$H = \frac{m}{2} \left[\dot{l}^2 + l^2 (\dot{\vartheta} + 1)^2 \right] + \frac{m}{2} [1 - 3 \cos^2(\vartheta)] \omega^2 l^2 + \frac{1}{2} K (l - l_0)^2 \quad (10)$$

Normalizing the Hamiltonian (i. e. dividing by $m \omega_0^2 l_0$), we obtain

$$h = \frac{1}{2} \left[\dot{l}^2 + l^2 (\dot{\vartheta} + 1)^2 \right] + \frac{1}{2} l^2 (1 - 3 \cos^2 \vartheta) + \frac{1}{2} k (l - 1)^2 \quad (11)$$

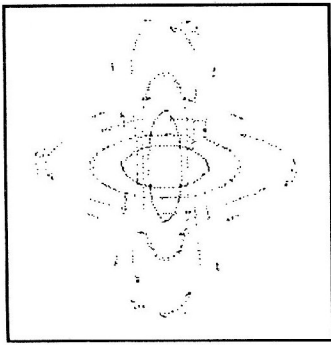
where: $k = K / m \omega_0^2$, and the dynamical equation can be written in canonical form

$$\begin{aligned} \dot{\vartheta} &= \frac{\partial h}{\partial p_\vartheta} = \frac{p_\vartheta}{l^2} \\ \dot{p}_\vartheta &= -\frac{\partial h}{\partial \vartheta} = -\frac{3}{2} l^2 \sin^2 \vartheta \\ \dot{l} &= \frac{\partial h}{\partial p_l} = p_l \\ \dot{p}_l &= -\frac{\partial h}{\partial l} = p_\vartheta^2 / l^3 - l(1 - 3 \cos^2 \vartheta) - k(l - 1) \end{aligned} \quad (12)$$

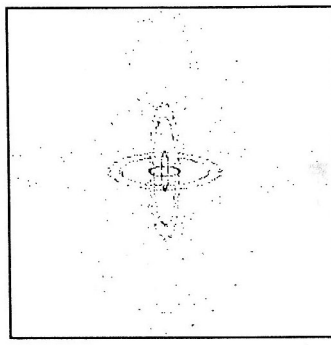
In what follows, equation (12) is numerically integrated for 4 different initial conditions, the Poincaré sections in the $(\vartheta - p_\vartheta)$ plane were obtained. The two different types of motion, regular and chaotic, are readily distinguished on the Poincaré maps, since for regular motion, successive points describe smooth curves or separate points; for chaotic motion, the points fill an area in an apparently random manner. In Figure 3a, for low energy level, most of the Poincaré maps are fairly well covered by invariant tori, that is, most of the periodic and quasiperiodic motions are preserved, as we go on increasing h , some tori break into chaotic trajectories (see Figure 3b - h), as h is further increased, more and more regular motion disappears, and finally ending in a chaotic ocean as shown in Figure 3f, g.

Literature

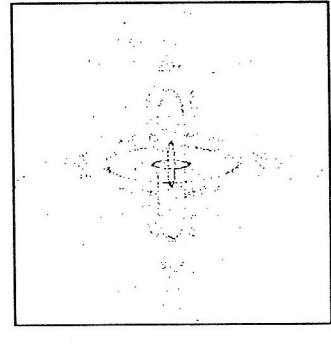
1. Liu, L.; Bainum, P. M.: Effect of Tether Flexibility on the Tethered Shuttle Subsatellite Stability and Control. *Journal of Guidance, Control, and Dynamics*, (1992), Vol. 12, No. 6, 866-873.
2. Bainum, P. M.; Kumar, V. K.: Optimal Control of the Shuttle-Tethered-Subsatellite System. *Acta Astronautica*, (1980), Vol. 7, 1333-1348.
3. Tong, X.; Rimrott, F.P.J.: Numerical Studies on Chaotic Planar Motion of Satellites in an Elliptic Orbit. *Int. J. Chaos, Solitons, and Fractals*, (1991), 1, 179-186.
4. Tong, X.; Rimrott, F.P.J.: Chaotic Attitude Motion of Gyrostat satellites in a central Force Field. *Nonlinear Dynamics*, (1992).
5. Tong, X.: Chaotic Attitude Motion of Sattelites in the Central Gravitational Field. PH.D thesis of the University of Toronto, (1992).
6. Guckenheimer, J.; Holmes, P.: *Nonlinear Oscillations, Dynamical Systems, and Bifurcation of Vector Fields*. Springer-Verlag, (1983).



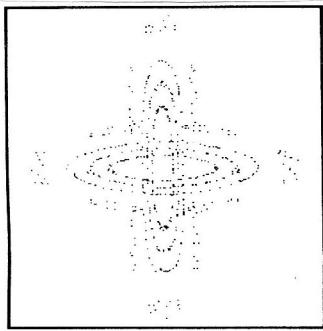
(a) $h = -1.25$



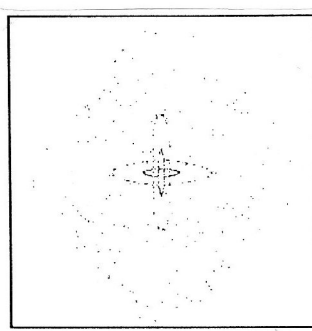
(b) $h = -0.75$



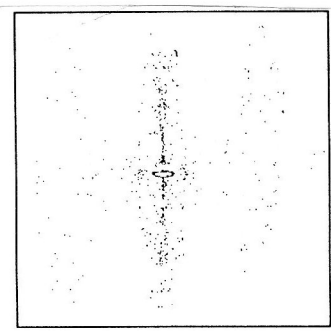
(c) $h = -0.6$



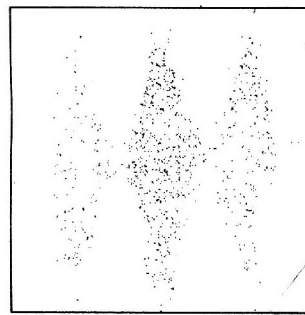
(d) $h = -0.6$



(e) $h = -0.5$



(f) $h = 0.0$



(g) $h = 0.5$

Figure 3. Poincaré maps of $\vartheta - p_\vartheta$ plane

Address: Dr. J. H. Peng, Professor Y. Z. Liu, Department of Engineering Mechanics, Shanghai Jiao Tong University, Shanghai 200030, P. R. China